

# Pairwise summation approximation for Casimir potentials and its limitations

Anne-Florence Bitbol,\* Antoine Canaguier-Durand,† Astrid Lambrecht, and Serge Reynaud  
*Laboratoire Kastler Brossel, ENS, UPMC, CNRS, F-75252 Paris, France*  
(Dated: November 1, 2012)

We investigate the error made by the pairwise summation (PWS) approximation in three geometries where the exact formula for the Casimir interaction is known: atom-slab, slab-slab and sphere-slab configurations. For each case the interactions are calculated analytically by summing the van der Waals interactions between the two objects. We show that the PWS result is incorrect even for an infinitely thin slab in the atom-slab configuration, because of local field effects, unless the material is infinitely dilute. In the experimentally relevant case of dielectric materials, in all considered geometries the error made by the PWS approximation is much higher than the well-known value obtained for perfect reflectors in the long-range regime. This error is maximized for permittivities close to the one of Silicon.

PACS numbers: 34.35.+a, 12.20Ds, 03.70.+k

## I. INTRODUCTION

The Casimir effect is the universal attraction between two perfectly reflecting plates in quantum vacuum due to the zero-point fluctuations of the electromagnetic field as first described in the seminal paper by Casimir<sup>1</sup>. A quantum mechanical treatment of van der Waals forces including the finite speed of light had already been established by Casimir and Polder shortly before by means of quantum electrodynamics<sup>2</sup>. It is therefore natural to wonder whether Casimir interactions between macroscopic objects can be deduced from the van der Waals interactions between their constituting atoms. A simple way of making this link would be to sum the van der Waals interactions between all pairs of constituting atoms, an approximation method known as *pairwise summation* (PWS). It is worth noting that attempts at explaining macroscopic interactions between colloids by pairwise summing van der Waals interactions were already carried out by de Boer and Hamaker<sup>3</sup> ten years before the work of Casimir and Polder.

However, the attractive PWS idea, that would reduce the Casimir effect – a physical effect of boundary conditions on the electromagnetic vacuum field – to a macroscopic resultant of two-body interatomic forces, has not been fundamentally successful. Indeed, PWS fails by construction to take into account any many-body effect. Such effects, for instance the screening of electromagnetic fields, are crucial in condensed matter physics, and have to be accounted for when computing the Casimir effect between macroscopic objects. Another fundamental cause of the insufficiency of PWS is the existence of three-body van der Waals-type interactions<sup>4</sup>. For permeable materials even the sign of the interaction can be erroneous when calculated within PWS<sup>5</sup>. Nevertheless, given the complexity of performing exact calculations of the Casimir effect in different geometries, the PWS approximation is still used nowadays since it provides approximations to the true Casimir interactions<sup>6–8</sup>. The results obtained by PWS are then often empirically renormalized by a corrective factor computed in a simpler case

where the exact Casimir interaction is known.

Limitations of PWS have been given in the past using a path integral formulation for fluctuation-induced forces to study the orientational dependence of PWS<sup>9</sup>, the force between deformed plates<sup>10</sup> or within a perturbative expansion in the dielectric contrast between arbitrarily shaped bodies<sup>11</sup>. Recently first principle calculations have obtained the PWS approximation as an asymptotic approximation of the Casimir energy in the weakly-coupled<sup>12</sup> or diluted limit<sup>13</sup>. In this paper, we investigate the error made by PWS using the scattering approach<sup>14–16</sup> in the atom-slab, slab-slab, and sphere-slab geometries, three fundamental geometries where the exact formula for the Casimir interaction is known. We investigate which effects cause the failure of the PWS approximation, and we study its error as a function of the material and the slab thickness. In Sec. II, the interactions between an atom and a slab, between two slabs and between a slab and a sphere are calculated analytically by PWS at any distance between the two interacting objects. Then, in Sec. III, the importance of local field effects as a cause of the failure of PWS is emphasized. The influence of the material for bulk mirrors and the effect of slab thickness in the long-range limit are studied in Sec. IV. We summarize our findings in Sec. V.

## II. PWS CALCULATION OF CASIMIR INTERACTIONS

PWS calculations are usually carried out in the short-range and long-range limiting regimes<sup>13,17–19</sup> where Casimir-Polder interactions reduce to power laws. For the sake of generality, we carry out the PWS calculation of the general Casimir-Polder interaction in order to obtain PWS estimates of the interactions between an atom and a slab, between two slabs, and between a sphere and a slab, at any distance between them. In these three well-known geometries, the PWS results can then be compared to the exact ones.

### A. Atom-slab geometry

We start from the van der Waals formula<sup>2</sup> giving the interaction energy between two atoms A and B of polarizabilities  $\alpha_A(\omega)$  and  $\alpha_B(\omega)$ , lying at a distance  $d$ :

$$U_{a-a}(d) = -\frac{\hbar c}{\pi d^2} \int_0^\infty du u^4 \frac{\alpha_A(\imath cu)\alpha_B(\imath cu)}{(4\pi\epsilon_0)^2} e^{-2ud} \times \left( \frac{3}{u^4 d^4} + \frac{6}{u^3 d^3} + \frac{5}{u^2 d^2} + \frac{2}{ud} + 1 \right) \quad (1)$$

where the integral is written over imaginary frequencies,  $\omega = \imath cu$ .

We then consider a slab of thickness  $e_A$  constituted of  $n_v^A$  atoms per unit volume at a distance  $L$  along the  $z$  axis from an isolated atom B (see Fig. 1).

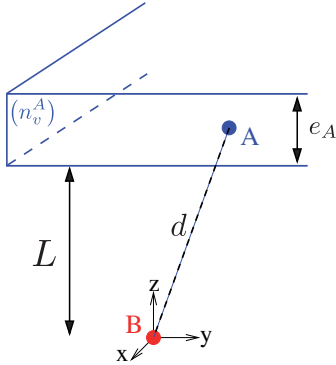


FIG. 1. Atom-slab geometry.

We compute the PWS interaction between the slab (s) and the atom (a) by summing the van der Waals interactions (1) between each atom A of the slab (s) and atom B:

$$U_{a-s}^{\text{PWS}}(L, e_A) = 2\pi n_v^A \int_L^{L+e_A} dz \int_0^\infty dr r U_{a-a}(d) \quad (2)$$

where  $d = \sqrt{z^2 + r^2}$ . The integrations over  $r$  and  $z$  can be carried out by parts after inverting them with the integration over  $u$ , yielding the following result:

$$U_{a-s}^{\text{PWS}}(L, e_A) = \hbar c n_v^A \int_0^\infty du u^3 \frac{\alpha_A(\imath cu)\alpha_B(\imath cu)}{(4\pi\epsilon_0)^2} \times [f(2uL) - f(2u(L+e_A))] \quad (3)$$

$$f(x) = x \Gamma(0, x) - e^{-x} \left( 1 + \frac{4}{x^2} + \frac{4}{x^3} \right),$$

$\Gamma$  being the incomplete Gamma function  $\Gamma : (a, x) \mapsto \int_x^\infty dt t^{a-1} e^{-t}$ .

A limiting case is the infinitely thick slab ( $e_A \rightarrow \infty$ ), corresponding to a bulk material. We will call this situation atom (a)- bulk plate (p) configuration in the remainder of the paper. For this geometry we obtain the

following interaction potential within PWS:

$$U_{a-p}^{\text{PWS}}(L) = \hbar c n_v^A \int_0^\infty du u^3 \frac{\alpha_A(\imath cu)\alpha_B(\imath cu)}{(4\pi\epsilon_0)^2} f(2uL). \quad (4)$$

### B. Slab-slab geometry

In order to compute the PWS estimate of the Casimir interaction between two slabs, we simply sum the previous result (3) over atoms B constituting another slab with thickness  $e_B$  and number of atoms per unit volume  $n_v^B$  in the same way as before (see Fig. 2).

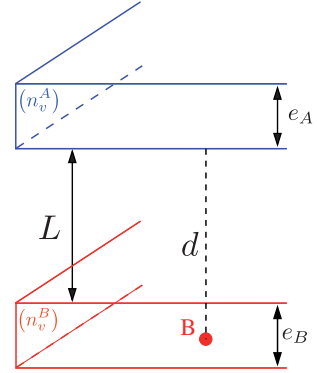


FIG. 2. Slab-slab geometry.

This procedure leads to the following PWS estimate of the Casimir interaction between two slabs of thicknesses  $e_A$  and  $e_B$  at a distance  $L$ , per unit surface:

$$U_{s-s}^{\text{PWS}}(L, e_A, e_B) = -\frac{\hbar c}{2} n_v^A n_v^B \int_0^\infty du u^2 \frac{\alpha_A(\imath cu)\alpha_B(\imath cu)}{(4\pi\epsilon_0)^2} \times [g(2uL) + g(2u(L+e_A+e_B)) - g(2u(L+e_A)) - g(2u(L+e_B))] \quad (5)$$

with

$$g(x) = \left( \frac{x^2}{2} - 2 \right) \Gamma(0, x) + e^{-x} \left( -\frac{x}{2} + \frac{1}{2} + \frac{2}{x} + \frac{2}{x^2} \right)$$

a primitive function of  $f(x)$  (see Appendix). When the slab thicknesses become infinitely large we obtain for the interaction between two bulk plates:

$$U_{p-p}^{\text{PWS}}(L) = -\frac{\hbar c}{2} n_v^A n_v^B \int_0^\infty du u^2 \frac{\alpha_A(\imath cu)\alpha_B(\imath cu)}{(4\pi\epsilon_0)^2} g(2uL). \quad (6)$$

### C. Sphere-slab geometry

We next consider a third experimentally relevant situation where object A is (again) a slab of thickness  $e_A$  and density  $n_v^A$ , while object B is a sphere of radius  $R$

and density  $n_v^B$ .  $L$  is the surface-surface distance of the two objects, while  $\mathcal{L}$  will be the center-to-plate distance ( $\mathcal{L} = L + R$ ) (see Fig. 3).

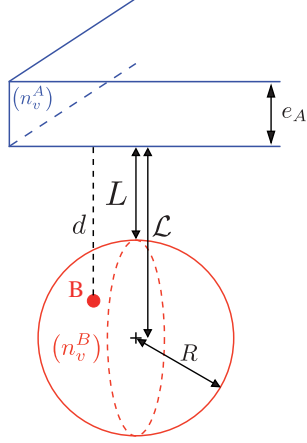


FIG. 3. Sphere-slab geometry.

We compute the interaction between the two objects by summing the atom-slab result given by Eq.(3) for each atom of the sphere  $B$  which lies at a distance  $d = \mathcal{L} + r$  from the slab, with  $r \in [-R, R]$ :

$$U_{sph-s}^{PWS}(\mathcal{L}, e_A) = \int_{-R}^R dr \ (\pi(R^2 - r^2)n_v^B) U_{a-s}^{PWS}(\mathcal{L} + r, e_A) \quad (7)$$

After several integration by parts, it is possible to show that the energy reads:

$$\begin{aligned} U_{sph-s}^{PWS}(\mathcal{L}, e_A) = & -\frac{\hbar c \pi}{4} n_v^A n_v^B \int_0^\infty du \ \frac{\alpha_A(\imath cu) \alpha_B(\imath cu)}{(4\pi\epsilon_0)^2} \\ & \times \{2uR[h(2u(\mathcal{L} + e_A + R)) + h(2u(\mathcal{L} + e_A - R)) \\ & - h(2u(\mathcal{L} + R)) - h(2u(\mathcal{L} - R))] \\ & - [i(2u(\mathcal{L} + e_A + R)) - i(2u(\mathcal{L} + e_A - R)) \\ & - i(2u(\mathcal{L} + R)) + i(2u(\mathcal{L} - R))]\} \end{aligned} \quad (8)$$

with

$$\begin{aligned} h(x) &= \left(\frac{x^3}{6} - 2t\right) \Gamma(0, x) + e^{-x} \left(-\frac{x^2}{6} + \frac{x}{6} + \frac{5}{3} - \frac{2}{x}\right) \\ i(x) &= \left(\frac{x^4}{24} - x^2 + 2\right) \Gamma(0, x) \\ &+ e^{-x} \left(-\frac{x^3}{24} + \frac{x^2}{24} + \frac{11x}{12} - \frac{3}{4}\right) \end{aligned}$$

two successive primitives of  $g(x)$  (see Appendix). In the limiting case of  $e_A \rightarrow \infty$ , we obtain:

$$\begin{aligned} U_{sph-p}^{PWS}(\mathcal{L}) = & \frac{\hbar c \pi}{4} n_v^A n_v^B \int_0^\infty du \ \frac{\alpha_A(\imath cu) \alpha_B(\imath cu)}{(4\pi\epsilon_0)^2} \\ & \times \{2uR[h(2u(\mathcal{L} + R)) + h(2u(\mathcal{L} - R))] \\ & - i(2u(\mathcal{L} + R)) + i(2u(\mathcal{L} - R))\} \end{aligned} \quad (9)$$

### III. LOCAL FIELD EFFECTS AND PWS

In Sec. II A, we calculated the PWS estimate of the atom-slab interaction by direct summation of the van der Waals atom-atom interactions. We now show that the same result can be derived within the scattering approach, which will make it easier to compare analytically the PWS result and the exact Casimir interaction in the atom-slab geometry.

#### A. Equivalence between PWS and the summation of reflection matrices

The Casimir interaction at zero temperature between any two objects  $A$  and  $B$  at a distance  $R$  along  $z$  from one another can be expressed as follows within the scattering approach to Casimir forces<sup>14–16</sup>:

$$U(R) = -\frac{\hbar c}{2\pi} \int_0^\infty du \ \text{Tr} \ln (\mathbf{1} - \mathcal{R}_B e^{-\mathcal{K}R} \mathcal{R}_A e^{-\mathcal{K}R}) \quad (10)$$

In this formula,  $\mathcal{R}_A$  and  $\mathcal{R}_B$  are the reflection matrices of the two interacting objects, while the two  $e^{-\mathcal{K}R}$  factors are propagation matrices. The term  $\mathcal{R}_B e^{-\mathcal{K}R} \mathcal{R}_A e^{-\mathcal{K}R}$  therefore corresponds to a complete roundtrip of the vacuum field between the two objects  $A$  and  $B$ : the field propagates from  $B$  to  $A$  before being reflected by  $A$ , then it propagates back to  $B$  and is reflected by  $B$ . The integration is on imaginary frequencies  $\omega = \imath cu$  of the electromagnetic field, while the trace  $\text{Tr}$  runs over all independent field modes at a given frequency  $\omega = \imath cu$ . Therefore, this formula takes into account the contribution of every electromagnetic mode to the Casimir effect.

If one of the objects is an atom, only a small fraction of the field is scattered back to object  $B$  and we may safely neglect multiple reflections. Thus, if  $A$  or  $B$  – or both – are atoms, the general formula (10) can be used at first order in  $\mathcal{R}_B e^{-\mathcal{K}R} \mathcal{R}_A e^{-\mathcal{K}R}$ , reducing to:

$$U(R) = -\frac{\hbar c}{2\pi} \int_0^\infty du \ \text{Tr} (\mathcal{R}_B e^{-\mathcal{K}R} \mathcal{R}_A e^{-\mathcal{K}R}) \quad (11)$$

In particular, inserting the expressions of atom reflection matrices (13) into the general Casimir interaction formula at first order (11) gives the van der Waals interaction between two atoms (1).

Let us now consider, as in Sec. II A, the case of an isolated atom  $B$  in front of a slab constituted of atoms  $A$  (see Fig. 1). Since formula (11) is linear in  $\mathcal{R}_A$ , it is equivalent to carry out a pairwise summation of atom-atom interactions as in Sec. II A or to sum the reflection matrices of the constituting atoms in order to obtain the reflection matrix of the slab. More precisely, if we write the slab reflection matrix as  $\mathcal{R}_s = \sum_A \mathcal{R}_A(\vec{R}_A)$ , where  $\vec{R}_A$  is the position of each atom  $A$  of the slab (the isolated atom  $B$  being at the origin of coordinates), the atom-slab

interaction can be written using (11):

$$\begin{aligned} U_{a-s}(L) &= -\frac{\hbar c}{2\pi} \int_0^\infty du \text{Tr} \left( \mathcal{R}_B e^{-\kappa L} \sum_A \mathcal{R}_A(\vec{R}_A) e^{-\kappa L} \right) \\ &= -\frac{\hbar c}{2\pi} \sum_A \int_0^\infty du \text{Tr} \left( \mathcal{R}_B e^{-\kappa L} \mathcal{R}_A(\vec{R}_A) e^{-\kappa L} \right) \\ &= \sum_A U_{a-a}(R_A) . \end{aligned} \quad (12)$$

We thus obtain the predicted result. It can also be understood intuitively: summing the reflection matrices of the constituting atoms amounts to considering each atom of the slab as an independent scatterer. Each of these atoms then interacts independently with the isolated atom through the electromagnetic field in an equivalent manner to PWS.

### B. Calculation of slab reflection coefficients by summation of reflection matrices

Having established that PWS is equivalent to summing the atom reflection matrices in the atom-slab geometry, we will now compare the exact reflection coefficients of a slab to the reflection coefficients obtained by summing the reflection matrices of the constituting atoms. For this, let us first calculate explicitly the latter coefficients.

First, we write the position vector of an atom A of the slab as  $\vec{R}_A = (\vec{r}_A, z_A = L + \zeta_A)$ . Thus  $\zeta_A$  ranges from 0 to  $e_A$  (see Fig. 1), while  $\vec{r}_A \in \mathbb{R}^2$ . In order to compute  $\mathcal{R}_s = \sum_A \mathcal{R}_A(\vec{r}_A, L + \zeta_A)$ , we calculate a matrix element of  $\mathcal{R}_s$  in the plane wave basis. At a given frequency, each plane wave is characterized by its two-dimensional transverse (i.e. orthogonal to  $z$ ) wave vector  $\vec{k}$ , its longitudinal direction and its polarization  $p$ , transverse electric (TE) or magnetic (TM). This description is complete since the modulus of the longitudinal component  $k^z$  of the wave vector can be deduced from the relation  $\omega = c\sqrt{|\vec{k}|^2 + |k^z|^2}$ .

Let us choose two plane waves  $(\vec{k}_1, p_1)$  and  $(\vec{k}_2, p_2)$ , the first one with longitudinal component in the  $+$  direction along  $z$  and the second one with longitudinal component in the  $-$  direction along  $z$ . Their respective unit polarization vectors are therefore noted  $\hat{\epsilon}_p^+(\vec{k}_1)$  and  $\hat{\epsilon}_p^-(\vec{k}_2)$ . The matrix element taken between our two plane waves of the reflection matrix of an atom A at  $(\vec{0}, L)$  is<sup>20</sup>:

$$\langle \vec{k}_2, p_2 | \mathcal{R}_A | \vec{k}_1, p_1 \rangle = -\frac{u^2 \alpha_A(\omega u)}{2\kappa_2 \epsilon_0} \hat{\epsilon}_{p_2}^-(\vec{k}_2) \cdot \hat{\epsilon}_{p_1}^+(\vec{k}_1) . \quad (13)$$

In this formula,  $\kappa_2$  is defined as:  $|k_2^z| = \omega \kappa_2$ . We can write  $\langle \vec{k}_2, p_2 | \mathcal{R}_A(\vec{r}_A, L + \zeta_A) | \vec{k}_1, p_1 \rangle = \langle \vec{k}_2, p_2 | \mathcal{R}_A | \vec{k}_1, p_1 \rangle e^{-i(\vec{k}_2 - \vec{k}_1) \cdot \vec{r}_A} e^{-(\kappa_2 - \kappa_1) \zeta_A}$ , taking into account the field's propagation between  $(\vec{0}, L)$  and each atom A situated at  $(\vec{r}_A, z_A = L + \zeta_A)$ .

We are now able to compute the matrix element of  $\mathcal{R}_s = \sum_A \mathcal{R}_A(\vec{r}_A, L + \zeta_A)$  between the two plane waves:

$$\begin{aligned} \langle \vec{k}_2, p_2 | \mathcal{R}_s | \vec{k}_1, p_1 \rangle &= \sum_A \langle \vec{k}_2, p_2 | \mathcal{R}_A(\vec{r}_A, z_A) | \vec{k}_1, p_1 \rangle \\ &= n_v \langle \vec{k}_2, p_2 | \mathcal{R}_A | \vec{k}_1, p_1 \rangle \int_{\mathbb{R}^2} d\vec{r}_A e^{-i(\vec{k}_2 - \vec{k}_1) \cdot \vec{r}_A} \\ &\quad \int_0^{e_A} d\zeta_A e^{-(\kappa_2 - \kappa_1) \zeta_A} . \end{aligned} \quad (14)$$

Once the integrals are calculated and  $\langle \vec{k}_2, p_2 | \mathcal{R}_A | \vec{k}_1, p_1 \rangle$  is replaced by its explicit expression (13), it yields:

$$\begin{aligned} \langle \vec{k}_2, p_2 | \mathcal{R}_s | \vec{k}_1, p_1 \rangle &= n_v \frac{\pi u^2 \alpha_A(\omega u)}{(4\pi\epsilon_0) \kappa_1^2} \hat{\epsilon}_{p_2}^-(\vec{k}_2) \cdot \hat{\epsilon}_{p_1}^+(\vec{k}_1) \\ &\quad (2\pi)^2 \delta(\vec{k}_2 - \vec{k}_1) (e^{-2\kappa_1 e_A} - 1) \end{aligned} \quad (15)$$

The scalar products of polarization unit vectors can be easily calculated by writing down the explicit form of these vectors as a function of  $\vec{k}$  and  $k^z$ <sup>20</sup>. Thus,  $\hat{\epsilon}_{p_2}^-(\vec{k}_2) \cdot \hat{\epsilon}_{p_1}^+(\vec{k}_1) = 0$  if  $p_1 \neq p_2$ , while  $\hat{\epsilon}_{TE}^-(\vec{k}_1) \cdot \hat{\epsilon}_{TE}^+(\vec{k}_1) = 1$  and  $\hat{\epsilon}_{TM}^-(\vec{k}_1) \cdot \hat{\epsilon}_{TM}^+(\vec{k}_1) = -(1 + 2\frac{k_1^2}{u^2})$ . We finally obtain:

$$\begin{aligned} \langle \vec{k}_2, p_2 | \mathcal{R}_s | \vec{k}_1, p_1 \rangle &= (-1)^{\sigma(p_1)} (2\pi)^2 \delta(\vec{k}_2 - \vec{k}_1) \delta_{p_1 p_2} r^{p_1}(\vec{k}_1, u) \end{aligned} \quad (16)$$

where  $\sigma(TE) = 1$  and  $\sigma(TM) = -1$ , and where:

$$r_{\text{slab}}^{TE}(\vec{k}_1, u) = n_v \frac{\pi u^2 \alpha_A(\omega u)}{(4\pi\epsilon_0) \kappa_1^2} (e^{-2\kappa_1 e_A} - 1) \quad (17)$$

$$r_{\text{slab}}^{TM}(\vec{k}_1, u) = r^{TE}(\vec{k}_1, u) \cdot \left( 1 + 2\frac{k_1^2}{u^2} \right) . \quad (18)$$

Equation (16) is totally general since it reflects the invariance laws of specular reflection: the transverse wave vector is conserved by specular reflection (this arises from the  $x$  and  $y$  invariance of the system through Noether's theorem), and TM and TE polarization are eigenmodes of specular reflection.

On the contrary, the reflection coefficients (17) and (18) are specific to our summation approach. Using these coefficients instead of the exact ones to compute the atom-slab Casimir interaction is equivalent to using the PWS approximation. We have proven this formally in Sec. III A, and it is straightforward to verify it explicitly by calculating the atom-slab Casimir interaction using formula (11) with the form of  $\mathcal{R}_s$  we have just found: the result obtained is exactly the one obtained by PWS, i.e. (3).

### C. Comparison of the exact Casimir interaction and the PWS estimate in the atom-thin slab geometry

In order to gain some insight into the error made by PWS, we now compare the reflection coefficients calculated by summation in the previous section to the exact

ones. This is equivalent to comparing the exact Casimir interaction and the PWS estimate in the atom-slab geometry.

So as to obtain its exact reflection coefficients, the slab is considered as a quantum optical network obtained by piling up a vacuum/matter interface, propagation over a length  $e_A$  in matter and a matter/vacuum interface. Its transfer matrix is therefore the product of the transfer matrices of the three elementary networks constituting it. For a given polarization  $p=TE,TM$  the slab reflection coefficients can be obtained from its transfer matrix<sup>21</sup>.

$$r_{\text{slab}}^p = -\frac{\text{sh } \eta}{\text{sh}(\eta + \theta^p)}. \quad (19)$$

In this formula,  $\eta = e_A \kappa_m$  corresponds to propagation in the slab, with  $\kappa_m = \sqrt{\epsilon u^2 + k^2}$ , while  $\theta^{TE} = \ln\left(\frac{\kappa_m + \kappa}{\kappa_m - \kappa}\right)$  and  $\theta^{TM} = \ln\left(\frac{\kappa_m + \epsilon\kappa}{\epsilon\kappa - \kappa_m}\right)$  are linked to the Fresnel vacuum/matter reflection coefficients through the relation  $r^p = -e^{-\theta^p}$ . Here we have noted  $\imath\kappa = |k^z|$  the modulus of the longitudinal wave vector and  $k = |\vec{k}|$  the modulus of the transverse wave vector.

If the exact reflection coefficients (19) are used to calculate the atom-slab interaction from formula (11), the expression of the exact Casimir-Polder interaction is obtained<sup>20</sup>.

As both exact (19) and PWS (17-18) reflection coefficients are nonlinear function of the slab thickness  $e_A$ , we compare them in the case of a thin slab ( $e_A \rightarrow 0$ ). This limiting case is interesting since one reason generally invoked to explain the errors of PWS is that it fails to take into account the screening of the electromagnetic field. If screening was the only problem of PWS, this method would be most accurate for a thin slab.

A first order development in  $e_A$  of the reflection coefficients obtained by summation (17-18) gives:

$$r_{\text{slab}}^{TE}(\vec{k}, u) = -2\pi n_v e_A \frac{\alpha_A(\imath cu)}{4\pi\epsilon_0} \frac{u^2}{\kappa} \quad (20)$$

$$r_{\text{slab}}^{TM}(\vec{k}, u) = 2\pi n_v e_A \frac{\alpha_A(\imath cu)}{4\pi\epsilon_0} \frac{u^2}{\kappa} \left(1 + 2\frac{k^2}{u^2}\right). \quad (21)$$

Similarly, the exact reflection coefficients (19) become, at first order in  $e$ :

$$r_{\text{slab}}^{TE}(\vec{k}, u) = -\frac{e_A(\epsilon - 1)u^2}{2\kappa} \quad (22)$$

$$r_{\text{slab}}^{TM}(\vec{k}, u) = -\left(1 + \frac{\epsilon + 1}{\epsilon} \frac{k^2}{u^2}\right) \frac{e_A(\epsilon - 1)u^2}{2\kappa}. \quad (23)$$

We notice that, at first order in  $e_A$ , the two TE reflection coefficients (20) and (22) are identical only if  $\epsilon = 1 + 4\pi n_v \frac{\alpha_A(\imath cu)}{4\pi\epsilon_0}$ , while the two TM reflection coefficients (21) and (23) are identical only if  $\frac{\epsilon + 1}{\epsilon} = 2$ , that is to say if  $\epsilon - 1$  vanishes. Thus, we can say that PWS gives exact results in the atom-thin slab geometry only if  $\epsilon = 1 + 4\pi n_v \frac{\alpha_A(\imath cu)}{4\pi\epsilon_0}$  with  $4\pi n_v \frac{\alpha_A(\imath cu)}{4\pi\epsilon_0} \ll 1$ , that is to say only in the case when the material of the slab is infinitely diluted.

This condition found in the limit of thin slabs is very general. In fact it can proven to be sufficient for any slab thickness: the condition  $\epsilon(\imath cu) = 1 + 4\pi n_v \frac{\alpha(\imath cu)}{4\pi\epsilon_0}$  with  $4\pi n_v \frac{\alpha(\imath cu)}{4\pi\epsilon_0} \ll 1$  is the first-order approximation of the Clausius-Mossotti relation:

$$\frac{\epsilon(\imath cu) - 1}{\epsilon(\imath cu) + 2} = \frac{4\pi}{3} n_v \frac{\alpha(\imath cu)}{4\pi\epsilon_0} \quad (24)$$

when  $n_v \alpha(\imath cu)$  is very small, i.e. at the diluted limit. If we insert this first-order approximation to the Clausius-Mossotti relation in the exact reflection coefficients (19), we obtain the reflection coefficients found by summation (17-18) for any slab thickness.

Replacing the Clausius-Mossotti relation by its first-order approximation amounts to neglecting local field effects. Therefore our analysis indicates that local field effects are crucial in the errors made by PWS. Moreover, the fact that the condition of validity of PWS is not more restrictive for a thick slab than for a very thin one suggests that screening is not the most important of the effects that cause the errors of PWS.

#### IV. INFLUENCE OF THE MATERIAL IN THE LONG-RANGE LIMIT

The formal comparison of the Casimir interaction and its PWS estimate in the atom-slab geometry has enabled us to gain some insight into the reasons why PWS is not exact, emphasizing the role of local field effects among the different many-body effects that are not taken into account in PWS. However, such formal comparisons are quite difficult to carry out in general, and it is of great practical importance to know the magnitude of the error made by approximations such as PWS.

The results that are generally cited about the errors of PWS involve perfect reflectors<sup>17,18</sup>. In the long-range (retarded) limit, the ratio between the pairwise approximation and the exact value of the atom-slab interaction is 1.15 if the slab is a perfect reflector. In the slab-slab geometry, this ratio is 0.80<sup>17</sup>. As the perfect reflector is an idealization, we may wonder how this ratio changes for real materials. In this section, we estimate numerically the ratio between the pairwise approximation and the exact value of the Casimir interaction for dielectric materials in the atom-slab and slab-slab geometries. In order to achieve model-independent results we restrict ourselves to the long-range limit.

##### A. Atom-slab interaction

Let us in a first step suppose that the slab thickness  $e_A$  is much larger than  $L$ . The influence of the slab thickness will be addressed later-on.

Besides we suppose that the distance  $L$  between the atom and the slab is much larger than any relevant intrinsic characteristic distance, such as the wavelengths

corresponding to the atomic transitions of the isolated atom, and any wavelength characteristic of the permittivity of the slab material. Practically, for a typical atom and a silicon slab with permittivity modeled by a Drude-Lorentz formula<sup>22</sup>, this means that  $L > 1 \mu\text{m}$ .

The exact atom-bulk plate interaction can be expressed thanks to formula (11), where  $\mathcal{R}_P$  is the slab reflection matrix (16) with the exact reflection coefficients (19). The latter reduce to the bulk Fresnel reflection coefficients, since we are dealing with infinite slabs. The result reads<sup>20</sup>:

$$U_{a-p}(L) = \frac{\hbar c}{2\pi} \int_0^\infty du u^2 \frac{\alpha_B(\imath cu)}{4\pi\epsilon_0} \int_u^\infty d\kappa e^{-2\kappa L} \left( r^{TE} + \left( 2\frac{\kappa^2}{u^2} - 1 \right) r^{TM} \right) \quad (25)$$

where  $r^{TE} = \frac{\kappa - \kappa_m}{\kappa + \kappa_m}$  and  $r^{TM} = \frac{\kappa_m - \epsilon\kappa}{\epsilon\kappa + \kappa_m}$ , with  $\kappa_m = \sqrt{u^2\epsilon(\imath cu) + k^2}$ . In the long-distance limit, the propagation factor  $e^{-2\kappa L}$  in the atom-plate Casimir interaction formula (25) vanishes except at small frequencies  $\omega = \imath cu$ , so that the polarizability of the isolated atom  $\alpha_B(\imath cu)$  and the permittivity  $\epsilon(\imath cu)$  can be replaced by their static values  $\alpha_B(0)$  and  $\epsilon(0)$ .

In the PWS approximation, the interaction will thus be given by formula (4). As before, the propagation factor  $e^{-2uL}$  allows for replacement of  $\alpha_A(\imath cu)$  and  $\alpha_B(\imath cu)$  by  $\alpha_A(0)$  and  $\alpha_B(0)$  in this formula in the long distance limit. Explicit integration then shows that formula (4) reduces to:

$$U_{a-p}^{\text{PWS}}(L) = -\frac{23}{40} \frac{\hbar c n_v^A}{L^4} \frac{\alpha_A(0)\alpha_B(0)}{(4\pi\epsilon_0)^2}. \quad (26)$$

This long-distance limit of formula (4) can be found by simple pairwise summation of the retarded Casimir-Polder interaction<sup>17</sup>.

We notice that in the long-distance limit,  $\alpha_B(0)$  is a simple multiplicative factor in both the exact Casimir interaction and its PWS estimate. Therefore, in this limit, the ratio  $U_{a-p}^{\text{PWS}}/U_{a-p}$  does not depend on any property of the isolated atom. Besides, in order to compare the PWS estimate to the exact Casimir interaction,  $\alpha_A(0)$  is expressed as a function of  $\epsilon(0)$  thanks to the Clausius-Mossotti relation (24).

It is now possible to compute the ratio  $U_{a-p}^{\text{PWS}}/U_{a-p}$  in the long range limit as a function of the only remaining material parameter  $\epsilon(0)$ . The result obtained is traced in Fig. 4.

We observe on Fig. 4 that the PWS method becomes correct when  $\epsilon(0) \rightarrow 1$ , that is to say when the bulk matter becomes infinitely diluted. This is consistent with the conclusions of Sec. III. Besides, we find the well-known result  $U_{a-p}^{\text{PWS}}/U_{a-p} = \frac{23}{20} \simeq 1.15$  corresponding to the perfect reflector in the limit  $\epsilon(0) \rightarrow \infty$ <sup>17,18</sup>. An unexpected and interesting result is that the ratio  $U_{a-p}^{\text{PWS}}/U_{a-p}$  does not evolve monotonically between these two limits, but has a maximum at  $\epsilon(0) \simeq 14.9$ , where

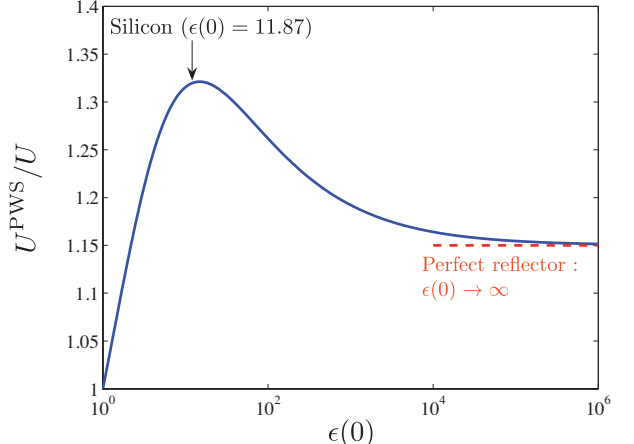


FIG. 4. Ratio of the PWS estimate of the atom-plate Casimir interaction and its exact value in the long-range limit. This ratio is traced as a function of the static permittivity.

$U_{a-p}^{\text{PWS}}/U_{a-p} \simeq 1.321$ . Moreover, this maximum corresponds to realistic dielectric materials. For instance, we show on Fig. 4 that silicon is very close to it, with  $\epsilon(0) = 11.87$  and  $U_{a-p}^{\text{PWS}}/U_{a-p} \simeq 1.319$ . PWS thus makes a larger error for dielectrics such as silicon than for a perfect reflector if the atom-bulk plate interaction is considered. The relative error can reach about 30%.

We now consider a finite thickness  $e_A$  for the slab and study its effect on the accuracy of the PWS method. We start from the derived expression (3) for the energy between the slab and the atom, and then apply the long-distance limit so that the polarizability of the isolated atoms can be replaced by their static values. It leads to a result similar to the bulk case (26), except for a thickness-dependent factor:

$$U_{a-s}^{\text{PWS}}(L, e_A) = U_{a-p}^{\text{PWS}}(L) \left( 1 - \frac{1}{\left( 1 + \frac{e_A}{L} \right)^4} \right). \quad (27)$$

For the computation of the exact Casimir energy, we use Eq.(25) with the thickness-dependent Fresnel coefficients introduced in Eq.(19). The obtained ratio is traced in Fig. 5 for various values of the relative thickness  $e = e_A/L$  which is dimensionless. We observe that the ratio of the PWS estimation over the exact result is also strongly dependent on the thickness of the slab compared to the distance between the two objects: while for a large thickness compared to the distance ( $e \gg 1$ ) the bulk plate case is recovered for any static permittivity, the ratio decreases dramatically when the thickness decreases. At the limit of infinite permittivity, or perfectly reflecting objects, the ratio goes as expected to the thickness-dependent ratio  $\left( 1 - (1 + e_A/L)^{-4} \right)$ .

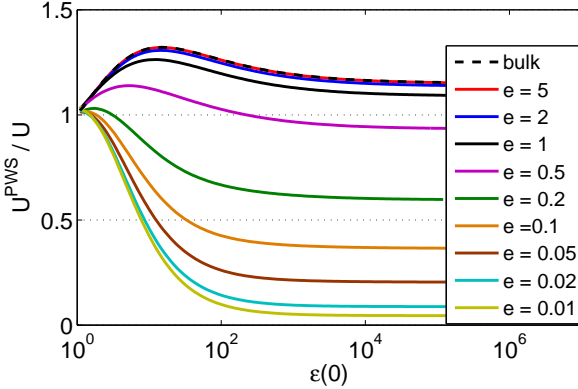


FIG. 5. Ratio of the PWS estimate of the atom-slab Casimir interaction and its exact value in the long-range limit, for various values of the relative thickness  $e = e_A/L$ . The case of a bulk plane is recalled with a dashed-line.

### B. Two slabs

Let us now carry out the same study for two bulk materials. In this geometry, the whole formula (10) has to be used since multiple reflections are not negligible. Using equation (16) for the reflection matrix of each plate, this formula gives the energy per unit area:

$$U_{p-p}(L) = \frac{\hbar c}{2\pi} \int_0^\infty du \operatorname{Tr} \ln (1 - r_B r_A e^{-2\kappa L}) \quad (28)$$

This formula is only valid for specular reflection. The general formula (10) for the Casimir interaction between any two objects was in fact first obtained as a generalization of the specific formula (28)<sup>15</sup>. After writing explicitly the trace over field modes, formula (28) becomes:

$$U_{p-p}(L) = \frac{\hbar c}{4\pi^2} \int_0^\infty du \int_u^\infty d\kappa \kappa \left[ \ln (1 - (r^{TE})^2 e^{-2\kappa L}) + \ln (1 - (r^{TM})^2 e^{-2\kappa L}) \right] \quad (29)$$

with the bulk reflection coefficients  $r^{TE}$  and  $r^{TM}$  such as defined after eqn. (25). We have assumed here that both plates are identical. In the case of perfect reflectors ( $r^2 = 1$ ), formula (29) reduces after some calculations to the original Casimir formula<sup>1</sup>  $U_{p-p}(L) = -\frac{\hbar c \pi^2}{720 L^3}$ .

In the PWS approximation, the interaction between two plates at any distance has been computed in Sec. II, formula (6). In the long distance limit the polarizabilities can be replaced by their static values, so that the general PWS result (6) can be simplified:

$$U_{p-p}^{\text{PWS}}(L) = -\frac{23}{120} \frac{\hbar c n_v^A n_v^B}{L^3} \frac{\alpha_A(0) \alpha_B(0)}{(4\pi\epsilon_0)^2} \quad (30)$$

This long-distance limit of formula (6) can also be found by simple pairwise summation of the retarded Casimir-Polder interaction<sup>17</sup>. Here we have  $\alpha_A = \alpha_B$  and  $n_v^A = n_v^B$  since both plates are supposed to be identical.

In order to compare the exact Casimir interaction and its PWS estimate, we use once more the Clausius-Mossotti relation (24) to express  $\alpha(0)$  as a function of  $\epsilon(0)$ . We now compute the ratio  $U_{p-p}^{\text{PWS}}/U_{p-p}$  in the long range limit using the same method as in the previous section. The result obtained is traced as a function of  $\epsilon(0)$  in Fig. 6.

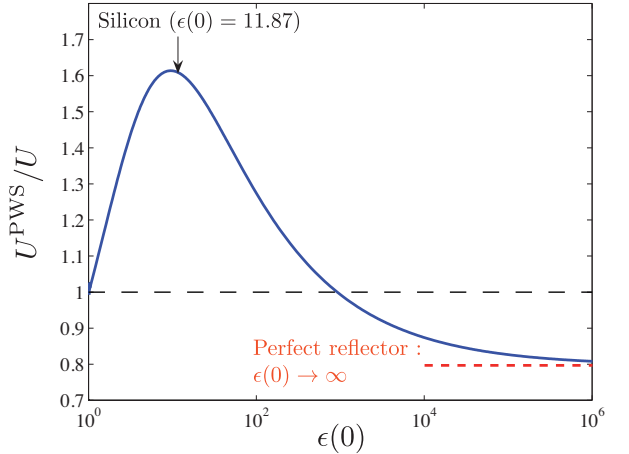


FIG. 6. Ratio of the PWS estimate of the plate-plate Casimir interaction and its exact value in the long-range limit. This ratio is traced as a function of the material's static permittivity.

While the global aspect of the ratio  $U_{p-p}^{\text{PWS}}/U_{p-p}$  in Fig. 6 is similar to the one plotted in Fig. 4 (atom-bulk plate interaction), the error of PWS in the two plates geometry is found to be twice as large, reaching now up to 60%.

Moreover, a striking feature in Fig. 6 is that the ratio  $U_{p-p}^{\text{PWS}}/U_{p-p}$  is larger than one for most dielectric materials ( $\epsilon(0) \lesssim 100$ ), while it is smaller than one for the perfect reflector ( $U_{p-p}^{\text{PWS}}/U_{p-p} = \frac{621}{8\pi^4} \simeq 0.797$ ). Thus, the perfect reflector result does not provide a correct explanation as to the reasons of failure of PWS in most materials. This observation illustrates the complexity of the error made by PWS: the PWS estimate can be either smaller or larger than the exact Casimir interaction depending on the material for a given geometry. Furthermore, screening of electromagnetic fields by slab atoms turns out not be the main responsible for the error as we would then expect the ratio  $U_{p-p}^{\text{PWS}}/U_{p-p}$  to be larger than one for all values of  $\epsilon(0)$ , which is not the case here. As we have argued in Sec. III, local field effects seem to play a crucial part in this error.

We now consider finite thicknesses  $e_A, e_B$  for the slabs and study the effect of these parameters on the accuracy of the PWS method. We start from the derived expression (5) for the energy between the slabs, and then apply the long-distance limit so that the polarizability of the isolated atoms can be replaced by their static values. It leads to a result similar to the bulk case (32), except for

a thickness-dependent factor:

$$U_{s-s}^{\text{PWS}}(L, e_A, e_B) = U_{p-p}^{\text{PWS}}(L) \times \left( 1 - \frac{1}{(1 + \frac{e_A}{L})^3} - \frac{1}{(1 + \frac{e_B}{L})^3} + \frac{1}{(1 + \frac{e_A}{L} + \frac{e_B}{L})^3} \right). \quad (31)$$

For the computation of the exact Casimir energy, we use Eq.(29) with the thickness-dependent Fresnel coefficients introduced in Eq.(19). For simplicity we will only consider the case where  $e_A = e_B$ . The obtained ratio is traced in Fig. 7 for various values of the relative thickness  $e = e_A/L = e_B/L$ , as in the atom-slab case in Fig. 5.

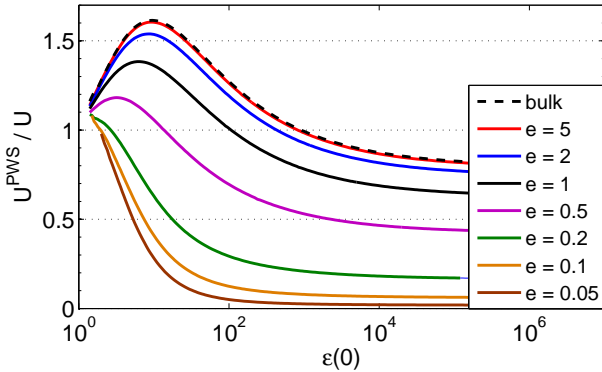


FIG. 7. Ratio of the PWS estimate of the slab-slab Casimir interaction and its exact value in the long-range limit, for various values of the relative thickness  $e = e_A/L = e_B/L$ . The case of two bulk planes is recalled with a dashed-line.

We observe that the ratio of the PWS estimation over the exact result is also strongly dependent on the thickness of the slabs compared to the distance between them: while for a large thickness compared to the distance ( $e \gg 1$ ) the bulk plate case is recovered for any static permittivity, the ratio decreases dramatically when the thickness decreases. At the limit of infinite permittivity, or perfectly reflecting objects, the ratio goes as expected to the thickness-dependent ratio  $(1 - 2(1+e)^{-3} + (1+2e)^{-3})$ .

### C. Sphere-bulk plate geometry

We finish this study with the sphere-slab configuration, where a sphere of radius  $R$  has its center at a distance  $\mathcal{L}$  from an infinitely thick slab. In this geometry the exact quantity for the Casimir energy  $U_{sph-p}$  has to be derived from the general scattering formula (10), with  $\mathcal{R}_S$  and  $\mathcal{R}_P$  the reflection operators on the sphere and on the plane, respectively. These operators can be expressed thanks to the bases of planar and spherical waves, as discussed in details in<sup>23,24</sup>. In the present study, we consider the long-range limit, in the sense that the distance

between the sphere and the infinite slab  $L = \mathcal{L} - R$  is much larger than any wavelength  $\lambda$  characteristic of the permittivity  $\epsilon$  of the objects material. As in the previous cases the permittivity and polarizability in the reflection operators  $\mathcal{R}_S$  and  $\mathcal{R}_P$  can then be replaced by their static value  $\epsilon(0)$ .

In the PWS approximation, the interaction between a sphere and a plate has been computed in Sec. II, formula (9). In the long-range limit the general PWS result (9) can be simplified to:

$$U_{sph-p}^{\text{PWS}}(L) = -\frac{23}{30} \frac{\hbar c \pi R^3 n_v^A n_v^B}{(\mathcal{L}^2 - R^2)^2} \frac{\alpha_A(0) \alpha_B(0)}{(4\pi\epsilon_0)^2} \quad (32)$$

Here we have  $\alpha_A = \alpha_B$  and  $n_v^A = n_v^B$  since the materials for the sphere and the slab are supposed to be identical.

In order to compare the exact Casimir interaction and its PWS estimate, we use once more the Clausius-Mossotti relation (24) to express  $\alpha(0)$  as a function of  $\epsilon(0)$ . We now compute the ratio  $U_{sph-p}^{\text{PWS}}/U_{sph-p}$  in the long range limit using the same method as in the previous sections. The result obtained is traced as a function of  $\epsilon(0)$  in Fig. 6, for several values of the additional geometrical parameter  $\frac{L}{R}$ .

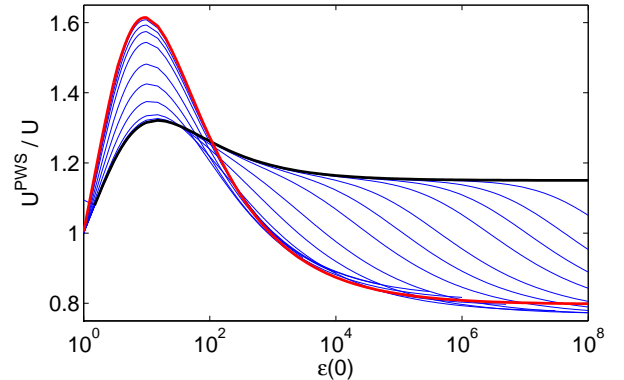


FIG. 8. Ratio of the PWS estimate of the sphere-slab Casimir interaction and its exact value in the case of infinitely thick slabs in the long-range limit, for various geometrical parameters  $\frac{L}{R}$  from 0.02 to 5000 (blue curves). This ratio is traced as a function of the static permittivity of the slab material. The black and red curves are a recall of the atom-slab and slab-slab cases, previously presented in Figs. 4 and 6, respectively.

The first observation is that the ratio  $U_{sph-p}^{\text{PWS}}/U_{sph-p}$  is dependent on the parameter  $\frac{L}{R}$ : for small values (i.e. very large spheres) this ratio tends to the plate-plate result, recalled by the red curve. On the opposite, for large values of  $\frac{L}{R}$  (i.e. small spheres) the curves converge to the atom-plate result, presented with a dark curve, except for very large values of  $\epsilon$ . Indeed, the small-sphere limit ( $R \ll L$ ) for perfect mirrors yields a ratio  $\frac{23}{30} \simeq 0.77$ , while the  $\epsilon(0) \rightarrow \infty$  limit for an atom in front of a slab leads to a ratio  $\frac{23}{20} = 1.15$ . This shows that the two limits

$(R \ll L)$  and  $(\epsilon(0) \rightarrow \infty)$ , of a small sphere and of a perfect reflector, do not commute. The ratio  $\frac{3}{2}$  is typical for this non-commutativity<sup>24</sup> and can be traced back to the small parameter-limit for the Mie coefficient  $b_\ell$ , or in other terms, to the impossibility to have a magnetic point-like dipole.

## V. CONCLUSION

We have investigated the error made by the pairwise summation method in three geometries where the exact formula for the Casimir interaction is known, the atom-slab, the slab-slab and the sphere-slab geometry. The scattering approach to the Casimir effect has enabled us to show, through an analytical comparison of reflection coefficients, that the PWS result is incorrect even for an infinitely thin slab interacting with an atom, unless the material is infinitely dilute. This analysis has stressed the fundamental importance of local field effects among the many-body effects that PWS fails to take into account.

We have then studied the influence of the material on the error made by PWS. This study has shown that the error made by the PWS method is much higher in the experimentally relevant case of dielectric materials such as silicon than for perfect reflectors. We have reached this conclusion in the long range limit, both in the atom-slab and in the slab-slab geometry. The existence of a maximum in the error made by PWS for the permittivity of usual dielectrics is not easy to understand intuitively and sheds light on the complexity of the error made by PWS. So does the fact that PWS can underestimate or overestimate the Casimir interaction in the slab-slab geometry depending on the slab permittivity. Although the error made by PWS is influenced by the slab thickness, in both geometries studied, it turns out to be no more accurate in the case of thin slabs than in the case of thick ones. This result confirms that the fact that PWS does not take into account the screening of electromagnetic fields cannot be the only explanation of the errors made by this method. For silicon slabs, PWS was found to underestimate or overestimate the Casimir interaction depending on the thickness in both geometries, showing once again the complexity of the error made by PWS.

## VI. ACKNOWLEDGEMENTS

The authors thank the ESF Research Networking Programme CASIMIR ([www.casimir-network.com](http://www.casimir-network.com)) for

providing excellent possibilities for discussions and exchange.

## Appendix A: Expressions for the successive primitive functions

The successive primitive functions involved in the derivations of the different energies are:

$$d(t) = -e^{-t} \left( \frac{1}{t} + \frac{4}{t^2} + \frac{20}{t^3} + \frac{48}{t^4} + \frac{48}{t^5} \right) \quad (A1)$$

$$e(t) = \Gamma(0, t) + 4e^{-t} \left( \frac{1}{t^2} + \frac{3}{t^3} + \frac{3}{t^4} \right) \quad (A2)$$

$$f(t) = t\Gamma(0, t) - e^{-t} \left( 1 + \frac{4}{t^2} + \frac{4}{t^3} \right) \quad (A3)$$

$$g(t) = \left( \frac{t^2}{2} - 2 \right) \Gamma(0, t) + e^{-t} \left( -\frac{t}{2} + \frac{1}{2} + \frac{2}{t} + \frac{2}{t^2} \right) \quad (A4)$$

$$h(t) = \left( \frac{t^3}{6} - 2t \right) \Gamma(0, t) + e^{-t} \left( -\frac{t^2}{6} + \frac{t}{6} + \frac{5}{3} - \frac{2}{t} \right) \quad (A5)$$

$$i(t) = \left( \frac{t^4}{24} - t^2 + 2 \right) \Gamma(0, t) + e^{-t} \left( -\frac{t^3}{24} + \frac{t^2}{24} + \frac{11t}{12} - \frac{3}{4} \right) \quad (A6)$$

$$j(t) = \left( \frac{t^5}{120} - \frac{t^3}{3} + 2t \right) \Gamma(0, t) + e^{-t} \left( -\frac{t^4}{120} + \frac{t^3}{120} + \frac{19t^2}{60} - \frac{17t}{60} - \frac{23}{15} \right) . \quad (A7)$$

All these functions vanish in the  $(t \rightarrow +\infty)$ -limit, and diverge in the  $(t \rightarrow 0)$ -limit, except the last one, for which  $j(0) = -\frac{23}{15}$ .

<sup>2</sup> H. Casimir and D. Polder, Physical Review, **73**, 360 (1948).

<sup>3</sup> H. Hamaker, Physica, **4**, 1058 (1937).

<sup>4</sup> B. M. Axilrod and E. Teller, Journal of Chemical Physics, **11**, 299 (1943).

<sup>\*</sup> Present address: Laboratoire Matière et Systèmes Complexes (MSC), CNRS UMR 7057, Université Paris Diderot

<sup>†</sup> Present address: ISIS - Université de Strasbourg.

<sup>1</sup> H. Casimir, Proceedings Koninklijke Nederlandse Akademie van Wetenschappen, **51**, 793 (1948).

<sup>5</sup> O. Kenneth, I. Klich, A. Mann, and M. Revzen, Physical Review Letters, **89**, 033001 (2002).

<sup>6</sup> H. G. Katzgraber, H. P. Büchler, and G. Blatter, Phys. Rev. B, **59**, 11990 (1999).

<sup>7</sup> X. Bouju, C. Joachim, and C. Girard, Phys. Rev. B, **50**, 7893 (1994).

<sup>8</sup> A. White and J. F. Dobson, Phys. Rev. B, **77**, 075436 (2008).

<sup>9</sup> R. Golestanian, Phys. Rev. E, **62**, 5242 (2000).

<sup>10</sup> T. Emig, A. Hanke, R. Golestanian, and M. Kardar, Phys. Rev. A, **67**, 022114 (2003).

<sup>11</sup> R. Golestanian, Phys. Rev. Lett., **95**, 230601 (2005).

<sup>12</sup> K. A. Milton, P. Parashar, and J. Wagner, Phys. Rev. Lett., **101**, 160402 (2008).

<sup>13</sup> P. Rodriguez-Lopez, Phys. Rev. E, **80**, 061128 (2009).

<sup>14</sup> M. Jaekel and S. Reynaud, Journal de Physique I, **1**, 1395 (1991).

<sup>15</sup> A. Lambrecht, P. A. Maia Neto, and S. Reynaud, New Journal of Physics, **8**, 243 (2006).

<sup>16</sup> T. Emig, N. Graham, R. L. Jaffe, and M. Kardar, Phys. Rev. Lett., **99**, 170403 (2007).

<sup>17</sup> P. Milonni, *The Quantum Vacuum - An Introduction to Quantum Electrodynamics* (Academic Press, 1994).

<sup>18</sup> V. Mostepanenko and N. Trunov, *The Casimir Effect and its Applications* (Clarendon Press - Oxford, 1997).

<sup>19</sup> V. B. Bezerra, G. L. Klimchitskaya, and C. Romero, Phys. Rev. A, **61**, 022115 (2000).

<sup>20</sup> R. Messina, D. Dalvit, P. A. Maia Neto, A. Lambrecht, and S. Reynaud, Phys. Rev. A, **80**, 022119 (2009).

<sup>21</sup> C. Genet, A. Lambrecht, and S. Reynaud, Phys. Rev. A, **67**, 043811 (2003).

<sup>22</sup> I. Pirozhenko and A. Lambrecht, Phys. Rev. A, **77**, 013811 (2008).

<sup>23</sup> P. A. Maia Neto, A. Lambrecht, and S. Reynaud, Phys. Rev. A, **78**, 012115 (2008).

<sup>24</sup> A. Canaguier-Durand, P. A. Maia Neto, A. Lambrecht, and S. Reynaud, Phys. Rev. A, **82**, 012511 (2010).